

ARTICLE

Open Access

LGK974 suppresses lipopolysaccharide-induced endotoxemia in mice by modulating the crosstalk between the Wnt/ β -catenin and NF- κ B pathways

Jaewoong Jang¹, Jaewon Song¹, Hyunji Lee¹, Inae Sim¹, Young V. Kwon², Eek-hoon Jho¹ and Yoosik Yoon¹

Abstract

Endotoxemia, a type of sepsis caused by gram-negative bacterial endotoxin [i.e., lipopolysaccharide (LPS)], is associated with manifestations such as cytokine storm; failure of multiple organs, including the liver; and a high mortality rate. We investigated the effect and mechanism of action of LGK974, a Wnt signaling inhibitor, in mice with LPS-induced endotoxemia, an animal model of sepsis. LGK974 significantly and dose-dependently increased the survival rate and reduced plasma cytokine levels in mice with LPS-induced endotoxemia. Transcriptome analysis of liver tissues revealed significant changes in the expression of genes associated with the Wnt pathway as well as cytokine and NF- κ B signaling during endotoxemia. LGK974 treatment suppressed the activation of NF- κ B signaling and cytokine expression as well as the Wnt/ β -catenin pathway in the livers of endotoxemic mice. Coimmunoprecipitation of phospho-I κ B and β -transducin repeat-containing protein (β -TrCP) was increased in the livers of endotoxemic mice but was reduced by LGK974 treatment. Moreover, LGK974 treatment decreased the coimmunoprecipitation and colocalization of β -catenin and NF- κ B, which were elevated in the livers of endotoxemic mice. Our results reveal crosstalk between the Wnt/ β -catenin and NF- κ B pathways via interactions between β -TrCP and phospho-I κ B and between β -catenin and NF- κ B during endotoxemia. The results of this study strongly suggest that the crosstalk between the Wnt/ β -catenin and NF- κ B pathways contributes to the mutual activation of these two pathways during endotoxemia, which results in amplified cytokine production, liver damage and death, and that LGK974 suppresses this vicious amplification cycle by reducing the crosstalk between these two pathways.

Introduction

Endotoxemia is mediated by the overproduction of proinflammatory cytokines caused by the endotoxin [i.e., lipopolysaccharide (LPS)] of gram-negative bacteria¹. Under normal physiological conditions, cytokine release is limited to regulate the immune response; however, the endotoxemic state induces unlimited cytokine production, a phenomenon termed “cytokine storm”. This phenomenon is mediated by the activation

of a cascade that induces autoamplification of cytokine production, which eventually results in multiple organ failure and death^{2,3}. Sepsis is defined as life-threatening organ dysfunction caused by a dysregulated host response to infection⁴, whereas endotoxemia is a type of sepsis-induced by infection with gram-negative bacteria⁵. The prevalence of endotoxemia is as high as to 82% in patients with sepsis⁶. Therefore, mice with LPS-induced endotoxemia have been used as an animal model of sepsis^{7–10}.

Liver dysfunction caused by bacteria and endotoxin is an essential event in sepsis accompanied by cytokine storm¹¹. Elevated cytokine expression in the liver is a marker of sepsis¹², and sepsis-induced liver dysfunction increases mortality¹³; therefore, attenuation of liver injury

Correspondence: Eek-hoon Jho (ej70@uos.ac.kr) or Yoosik Yoon (thanks@cau.ac.kr)

¹Department of Microbiology, Chung-Ang University College of Medicine, Seoul 06974, Republic of Korea

²Department of Biochemistry, University of Washington, Seattle, WA 98195, USA

Full list of author information is available at the end of the article

© The Author(s) 2021



Open Access This article is licensed under a Creative Commons Attribution 4.0 International License, which permits use, sharing, adaptation, distribution and reproduction in any medium or format, as long as you give appropriate credit to the original author(s) and the source, provide a link to the Creative Commons license, and indicate if changes were made. The images or other third party material in this article are included in the article's Creative Commons license, unless indicated otherwise in a credit line to the material. If material is not included in the article's Creative Commons license and your intended use is not permitted by statutory regulation or exceeds the permitted use, you will need to obtain permission directly from the copyright holder. To view a copy of this license, visit <http://creativecommons.org/licenses/by/4.0/>.

and restoration of liver function significantly lower the mortality risk of patients with sepsis¹⁴.

Recently, Wnt signaling has been reported to be involved in inflammation and sepsis. Microbial stimulation of human mononuclear cells induces WNT5A, which upregulates the expression of proinflammatory cytokines, including IL-6 and IL-1 β ¹⁵. An inhibitor of β -catenin-mediated transcription, iCRT3, was reported to reduce LPS-induced WNT signaling and proinflammatory cytokine production¹⁶. It was reported that WNT5A levels were significantly increased in the sera of patients with sepsis¹⁷ and that multiple WNT ligands were expressed in the peripheral blood of patients with septic shock¹⁸. However, the crosstalk between the Wnt/ β -catenin and NF- κ B pathways has not yet been elucidated in the context of sepsis. In this study, we analyzed the effects of LGK974, a Wnt signaling inhibitor, in LPS-induced endotoxemic mice through analyses of the crosstalk between the Wnt/ β -catenin and NF- κ B pathways in the liver as well as the effects of this crosstalk on the survival rate and induction of cytokine storm.

LGK974 has been developed as a candidate anticancer drug against Wnt-driven cancers¹⁹; it has shown suppressive effects against ovarian cancer²⁰, lung cancer²¹, squamous cell carcinoma^{22,23}, glioblastoma^{24,25}, and colon cancer²⁶. It is currently in phase I clinical trial in patients with colorectal cancer²⁷. Other effects of this Wnt signaling inhibitor have also been reported; LGK974 has been shown to ameliorate cystogenesis in a mouse model of polycystic kidney disease²⁸. We previously reported that LGK974 exerts anti-inflammatory effects in LPS-stimulated human bronchial epithelial cells and human umbilical vein endothelial cells²⁹. However, no studies have investigated its effects on sepsis. Sepsis is the most common cause of death among critically ill patients in noncoronary intensive care units, and there is an urgent need for an effective treatment for sepsis³⁰. Thus, in the present study, we examined the effect and mechanism of action of LGK974 in mice with LPS-induced endotoxemia, an animal model of sepsis.

Materials and methods

Reagents

Anti-I κ B (cat# 9242), anti-phospho-I κ B (Ser 32/36) (cat# 9246), anti-NF- κ B p65 (cat# 8242), anti-GSK3 β (cat# 9315), anti-phospho-GSK3 β (Ser 9) (cat# 9336), anti-AXIN (cat# 2087), anti-LRP6 (cat# 3395), anti-phospho-LRP6 (Ser 1490) (cat# 2568), and anti- β -TrCP (cat# 4394S) primary antibodies, as well as anti-mouse (cat# 7076S) and anti-rabbit (cat# 7074S) secondary antibodies, were purchased from Cell Signaling Technology (Danvers, MA, USA). An anti- β -catenin antibody (cat# 610153) was purchased from BD Transduction Laboratories Inc. (Lexington, KY, USA). Anti- β -actin (cat# 47778) and

anti-TBP (cat# 204) antibodies were purchased from Santa Cruz Biotechnology Inc. (Santa Cruz, CA, USA). LPS from *Klebsiella pneumoniae* was purchased from Sigma-Aldrich (St. Louis, MO, USA). LGK974 was obtained from MedChemExpress (Monmouth Junction, NJ, USA).

Animal experiments

Animal experimental protocols were approved by the institutional animal care and use committee of Chung-Ang University (approval numbers 2017-00099 and 2018-00042), and all experiments were performed in accordance with the animal research: reporting of in vivo experiments guidelines. Male C57BL/6 mice (4 weeks old) were purchased from Central Lab Animal Inc. (Seoul, Republic of Korea). LGK974 was injected *i.p.* 2 h before *i.p.* injection of LPS in most experiments. For survival experiments, various doses of LGK974 were injected 2 h before, simultaneously with, or 1 h after LPS injection. For another survival experiment, various doses of LGK974 were injected simultaneously with *Escherichia coli* (*E. coli*). *E. coli* strain K12 was cultured overnight in LB broth, and cell numbers were determined based on the optical density at 600 nm. Then, 10¹¹ colony-forming units (CFUs) of *E. coli* were resuspended in 200 μ l of saline immediately before *i.p.* injection. Both LGK974 and LPS were dissolved in saline by vigorous vortexing immediately before injection. Saline-injected mice served as a control group. Mice were anesthetized via *i.p.* injection of 10 mg/kg alfaxalone (Jurox, Rutherford, Australia) 6 h after LPS injection. Liver tissue was collected and stored at -70°C for further analyses. Blood samples were collected in EDTA tubes and were then centrifuged at 2000 $\times g$ for 10 min to collect plasma. A magnetic Luminex assay with antibody-based 9-plex immunoassays (Luminex, Austin, TX, USA) was used to measure the plasma concentrations of selected cytokines, including TNF- α , IL-6, IL-1 β , IL-1 α , IL-12, IFN- γ , MCP-1, RANTES, and IL-10. Measurements were performed using a Magpix Luminex instrument (Luminex) and MasterPlex QT 2010 software (MiraiBio, San Francisco, CA, USA).

RNA-seq and gene set enrichment analysis (GSEA)

RNA samples extracted from the livers of mice were analyzed by RNA-seq, and the original raw data have been deposited in the NCBI Gene Expression Omnibus database under accession number GSE127459 (<https://www.ncbi.nlm.nih.gov/geo/query/acc.cgi?acc=GSE127459>).

GSEA was conducted to compare the RNA-seq data sets. The primary result of GSEA is an enrichment score (ES), which indicates the degree to which a gene set is overrepresented among upregulated genes or downregulated genes in a ranked list of genes in the expression data set. A positive ES indicates enrichment of the gene

set among the upregulated genes in the ranked list; a negative ES indicates enrichment of the gene set among the downregulated genes in the ranked list. The normalized ES (NES) is the ES for the gene set after normalization across all analyzed gene sets. The significance (*P* value) of the NES is primarily affected by the false discovery rate, which is the probability that a gene set with a given NES represents a false-positive finding (<http://software.broadinstitute.org/gsea/index.jsp>)³¹.

Quantitative reverse-transcription (RT-q)PCR

Total RNA was isolated from liver tissue using an RNeasy Kit (Qiagen; Cat. No. 74106) in a homogenizer. One microgram of RNA was reverse transcribed using a cDNA Reverse Transcription Kit (Applied Biosystems Inc.; Cat. No. 43-688-13). RT-qPCR was conducted as described previously²⁹. Assay-on-Demand gene expression products (Applied Biosystems, Inc., Foster City, CA, USA) were used for RT-qPCR to evaluate the mRNA levels of *Tnf* (Mm00443258_m1), *Il6* (Mm00446190_m1), *Il1b* (Mm00434228_m1), *Il1a* (Mm00439620_m1), *Wnt3a* (Mm00437337_m1), *Wnt5a* (Mm00437347_m1), *Wnt10a* (Mm00437325_m1), and *Wnt10b* (Mm00442104_m1). For each experimental group, the mRNA levels were normalized to the 18S ribosomal RNA level, and the ratios of the normalized mRNA levels in each group were compared to those in the control group using the comparative Ct method³².

Protein extraction and western blotting

Liver tissues were lysed in a homogenizer using RIPA buffer containing 25 mM Tris-HCl (pH 7.6), 150 mM NaCl, 1% Nonidet P-40, 1% sodium deoxycholate, 0.1% sodium dodecyl sulfate, and protease inhibitor cocktail (Sigma-Aldrich; Cat. No. P8340) for 30 min at 4 °C. Total tissue lysates were obtained after removing the insoluble material by centrifugation at 20,000 × *g* for 20 min at 4 °C. Nuclear lysates were collected from liver tissue using a nuclear extraction kit (Active Motif, Carlsbad, CA, USA). Protein concentrations were determined using a BCA protein assay kit (Pierce, Waltham, MA, USA), and 10–100 µg of protein was analyzed by western blotting as described previously²⁹. β-Actin and TATA box-binding protein (TBP) were used as loading controls for total tissue lysates and nuclear lysates, respectively. Band intensities—corresponding to protein expression levels—were quantified by ImageJ (NIH, Bethesda, MD, USA) and normalized to those of the loading controls.

Target DNA-binding activity of NF-κB

Nuclear fractions were collected from frozen tissues using a nuclear extraction kit (Active Motif, Carlsbad, CA, USA), and protein concentrations were determined using a BCA protein assay kit (Pierce). The binding affinity of

NF-κB to its target DNA sequence (5'-GGGACTTCC-3') was measured using a TransAM NF-κB ELISA Kit (Active Motif) according to the manufacturer's instructions. Briefly, 10 µg of protein (nuclear fraction) was added to a 96-well plate coated with oligonucleotides containing the target DNA sequence. After incubation and washing, an anti-NF-κB antibody was added to the wells, followed by the horseradish peroxidase-conjugated secondary antibody provided in the kit. The absorbance at 450 nm was measured after sequential addition of the developing solution and the stop solution provided in the kit.

Coimmunoprecipitation assay for protein–protein binding interactions

Coimmunoprecipitation experiments were performed using an immunoprecipitation kit from BioVision (Mountain View, CA, USA) according to the manufacturer's instructions. Frozen tissues were lysed in a homogenizer using a nondenaturing lysis buffer provided in the kit at 4 °C for 30 min and were then centrifuged at 10,000 × *g* for 10 min at 4 °C. The supernatant was supplemented with 2 µg/ml of an antibody specific for the bait protein and incubated overnight at 4 °C. After adding 25 µl of protein A/G bead slurry and incubating for 1 h at 4 °C, the beads were collected by centrifugation at 2000 × *g* for 2 min. The collected beads were washed three times with 1 ml of wash buffer provided with the kit and mixed with 40 µl of 2× sodium dodecyl sulfate-polyacrylamide gel electrophoresis loading buffer. The amount of target protein bound to the beads was measured by western blotting with an antibody specific for the target protein. Band intensities were quantified using ImageJ (NIH, Bethesda, MD, USA).

Confocal microscopy for evaluation of protein colocalization

Tissue preparation and confocal microscopy were conducted as described previously with some modifications³³. Liver tissues were snap-frozen and embedded in OCT compound (Sakura, Tokyo, Japan). Embedded tissues were cryosectioned at a thickness of 10 µm. For immunofluorescence, sections were fixed with cold acetone for 10 min and incubated first in blocking buffer (CAS-Block; Thermo Fisher Scientific) for 1 h and then with a mouse anti-β-catenin antibody (Transduction Laboratory, #610153; 1:200) and a rabbit anti-NF-κB p65 antibody (Cell Signaling Technology #8242, 1:200) in phosphate-buffered saline (PBS) overnight. Sections were washed three times in PBS containing 0.03% Triton X-100 and incubated with a Cy3-labeled donkey anti-mouse IgG antibody (cat# 715-165-150, Jackson ImmunoResearch Laboratories, Inc., West Grove, PA, USA, 1:400) and FITC-labeled donkey anti-rabbit IgG (cat# 715-095-152,

Jackson ImmunoResearch Laboratories, Inc., 1:400) in PBS for 1 h. After counterstaining with 1 µg/ml DAPI (cat# D9542, Sigma-Aldrich), the tissues were mounted and visualized under a confocal microscope (Nikon A1Si, Nikon, Tokyo, Japan). Images from different experimental groups were acquired under the same exposure and detection settings. Colocalization of fluorescence signals was analyzed using ImageJ.

Statistical analysis

All data are expressed as the mean ± standard deviation values. Differences among experimental groups were analyzed using one-way ANOVA with Duncan's multiple range test. $P < 0.05$ was considered significant. All analyses were performed using SPSS ver. 14 (SPSS, Chicago, IL, USA).

Results and discussion

LPS-induced endotoxemic mice show dose-dependent lethality and cytokine storm

LPS decreased the survival rate of C57BL/6 mice in a dose-dependent manner (Fig. 1a). To evaluate whether LPS-induced endotoxemia induces cytokine storm in mice, the concentrations of plasma cytokines were measured after the injection of LPS at various doses (Fig. 1b–j). The plasma concentrations of TNF- α , IL-6, IL-1 β , IL-1 α , IL-12, INF- γ , MCP-1, RANTES, and IL-10 were markedly and dose-dependently increased in mice injected with 1–25 mg/kg LPS. As the highest plasma cytokine levels were observed after injection of 25 mg/kg LPS, this dose was used to induce endotoxemia in subsequent experiments.

LGK974 improves the survival rate and suppresses cytokine storm in mice with LPS-induced endotoxemia

We analyzed the effect of LGK974 on the survival rate of mice with LPS-induced endotoxemia (4-week-old male mice). The survival rate of mice that received 25 mg/kg LPS alone was 0%. Mice treated with 20 and 40 mg/kg LGK974 before LPS injection exhibited survival rates of 20 and 80%, respectively, whereas mice treated with 60 mg/kg LGK974 had a 100% survival rate (5 mice per group) (Fig. 2a). It should be noted that LGK974 increased the survival rate of mice with LPS-induced endotoxemia regardless of whether it was administered simultaneously with LPS injection (Fig. 2b) or after LPS injection (Fig. 2c). Moreover, LGK974 increased the survival rate of mice injected with viable *E. coli* cells (Fig. 2d). Overall, these results showed that LGK974 improved the survival rate of mice in which sepsis was induced by injection of endotoxin or bacteria in a dose-dependent manner. We also conducted survival experiments in 4-week-old female mice and 13-week-old male mice (Supplementary Data 1). LGK974 increased the survival rate in both experiments,

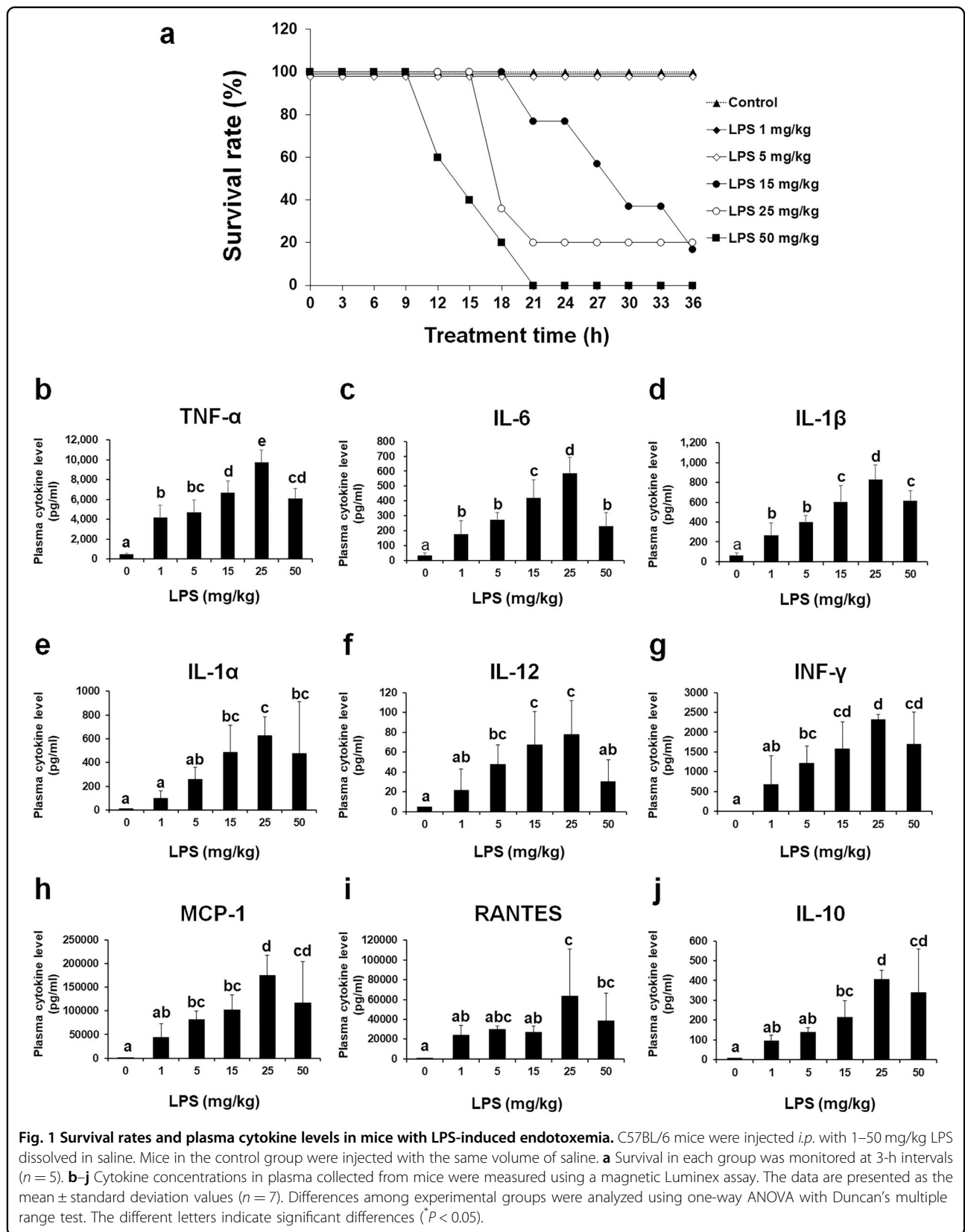
suggesting that the protective effect of LGK974 may be independent of the sex and age of the mice. The effects of LGK974 on mice older than 13 weeks remain to be investigated in further studies.

When mice were injected with 0–60 mg/kg LGK974 and 25 mg/kg LPS, the levels of proinflammatory cytokines, including TNF- α , IL-6, IL-1 β , IL-1 α , IL-12, INF- γ , MCP-1, and RANTES, were significantly and dose-dependently downregulated by LGK974 (Fig. 2e–l). However, the level of IL-10 was not altered upon LGK974 treatment (Fig. 2m). IL-10 is a potent anti-inflammatory cytokine that plays a central role in limiting the host immune response, thereby preventing damage to host tissues³⁴. The effects of LGK974 on other anti-inflammatory cytokines remain to be elucidated. Our data suggest that LGK974 has a suppressive effect on proinflammatory cytokine production in mice with LPS-induced endotoxemia.

RNA-seq and GSEA of liver tissue reveal significant changes in the expression of genes in the Wnt pathway as well as cytokine and NF- κ B signaling during LPS-induced endotoxemia

Among the multiple organs damaged in endotoxemia, we focused on the liver, as liver dysfunction caused by bacteria or endotoxin has been shown to be an essential event in sepsis, along with cytokine storm¹¹. RNA-seq experiments were conducted to analyze gene expression patterns in liver tissues from saline-injected mice (control group) and mice injected with 25 mg/kg LPS (endotoxemic group) or with 60 mg/kg LGK974 and 25 mg/kg LPS (LGK974 group). The complete set of RNA-seq data, including fold changes, P values, and expression levels for more than 23,000 genes, are presented in Supplementary Data 2 (RNA-seq data).

GSEA showed that many gene ontology (GO) terms related to cytokines, NF- κ B signaling, and the Wnt pathway were significantly altered in the liver upon LPS and LGK974 treatment; among these alterations, the changes in three GO terms are illustrated in Fig. 3, and the complete set of GSEA data for all GO terms is shown in Supplementary Data 3 (GSEA data). Most of the GO terms related to cytokine and NF- κ B signaling were overrepresented in the endotoxemic group compared with the control group. The GO terms “cytokine activity” and “I κ B kinase NF- κ B signaling” are illustrated in Fig. 3a, b. Among the GO terms related to the Wnt pathway, the GO term “negative regulation of Wnt signaling pathway” was significantly underrepresented (Fig. 3c), while the GO term “positive regulation of Wnt signaling pathway” was not significantly changed (Supplementary Data 3 (GSEA data)). The GO terms “cytokine activity” and “I κ B kinase NF- κ B signaling” were significantly underrepresented, whereas the GO term “negative regulation of Wnt



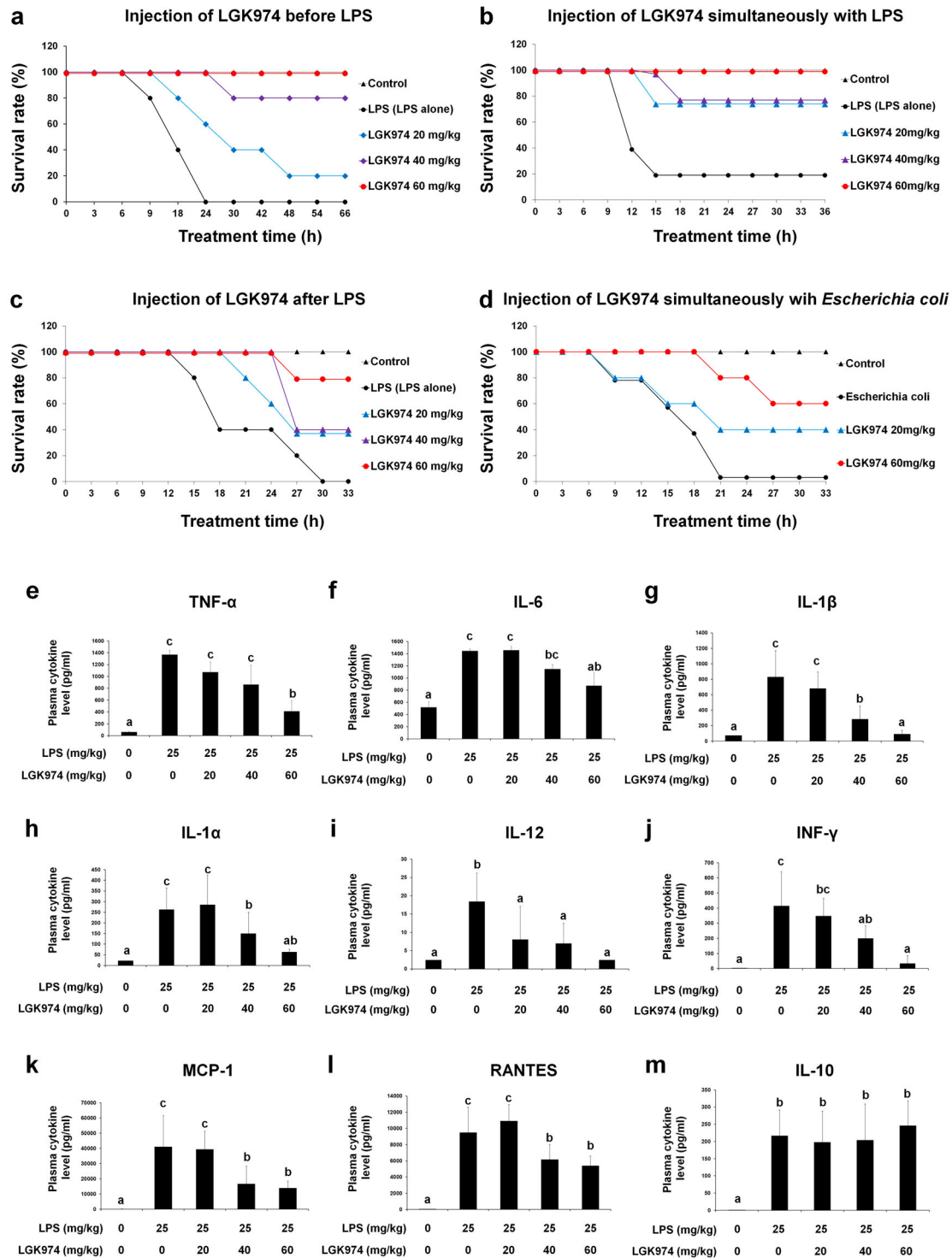
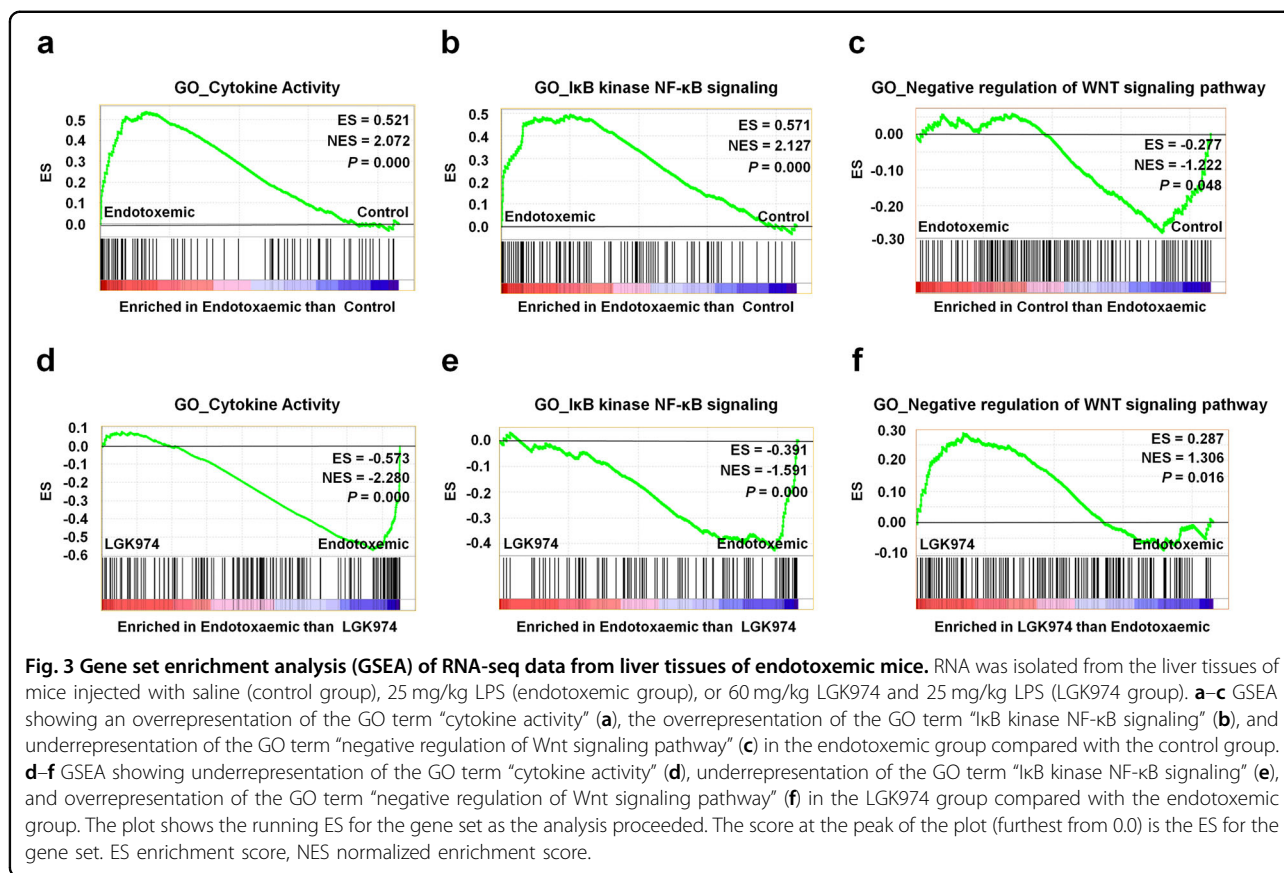


Fig. 2 Effect of LGK974 on the survival rate and cytokine storm in endotoxemic mice. **a–d** Effect of LGK974 on the survival rate in various endotoxemic mouse models ($n = 5$). LGK974 (0–60 mg/kg) was injected *i.p.* **a** 2 h before, **b** simultaneously with, and **c** 1 h after *i.p.* injection of 25 mg/kg of LPS. **d** LGK974 (0–60 mg/kg) was injected *i.p.* simultaneously with 10^{11} CFU of viable *Escherichia coli* cells. Mice in the control group were injected with the same volume of saline. **e–m** LGK974 suppresses cytokine storm in endotoxemic mice. C57BL/6 mice were injected *i.p.* with 0–60 mg/kg LGK974 2 h before being injected with 25 mg/kg LPS. Cytokine concentrations in the plasma were determined using a magnetic Luminex assay. The data are presented as the mean \pm standard deviation values ($n = 7$). Differences among experimental groups were analyzed using one-way ANOVA with Duncan’s multiple range test. The different letters indicate significant differences ($P < 0.05$).



signaling pathway” was significantly overrepresented in the LGK974 group compared with the endotoxemic group (Fig. 3d–f). The list of genes in these selected GO terms is shown in Supplementary Data 4 (List of genes in selected GO terms). Collectively, these results suggested that the levels of transcripts associated with the Wnt pathway as well as with NF-κB signaling and cytokines were significantly changed in the livers of LPS-induced endotoxemic mice and that these changes were suppressed by LGK974 treatment.

NF-κB signaling and cytokine expression are accompanied by Wnt signaling activation in the livers of mice with LPS-induced endotoxemia

To confirm the findings of RNA-seq and GSEA, western blot and RT-qPCR experiments were conducted. Proteins were extracted from the livers of mice injected with 0, 5, or 25 mg/kg LPS and analyzed by western blotting (Fig. 4a). All original western blot images are provided in Supplementary Data 5. In the livers of mice with LPS-induced endotoxemia, phosphorylation of IκB increased, whereas the amount of IκB decreased (Fig. 4a–c). Moreover, the nuclear levels of NF-κB (Fig. 4a, d) and the target DNA-binding activity of NF-κB (Fig. 4e) were increased. NF-κB is a major proinflammatory transcription factor

that binds to the regulatory region of genes encoding proinflammatory cytokines, thus inducing proinflammatory cytokine expression^{35,36}. The relative mRNA expression levels of *Tnf*, *Il6*, *Ilb*, and *Ila* (the genes encoding TNF-α, IL-6, IL-1β, and IL-1α, respectively) were significantly increased by LPS in a dose-dependent manner (Fig. 4f–i).

As the GSEA results suggested that Wnt signaling in the liver was significantly changed during endotoxemia, we analyzed this pathway in detail. The mRNA levels of Wnt genes such as *Wnt3a*, *Wnt5a*, *Wnt10a*, and *Wnt10b* were significantly increased by LPS in a dose-dependent manner (Fig. 4j–m). The protein levels of phospho-lipoprotein receptor-related protein 6 (LRP6) (Fig. 4n, o), and phospho-glycogen synthase kinase-3β (GSK-3β) (Fig. 4n), two positive regulators of Wnt signaling, were increased by LPS. Conversely, AXIN, a negative regulator of Wnt signaling, was downregulated (Fig. 4n, p). β-Catenin, the executor protein of Wnt signaling, was significantly upregulated (Fig. 4n, q). Similarly, the expression of β-transducin repeat-containing protein (β-TrCP), which is one of the target genes of β-catenin³⁷, was upregulated (Fig. 4n, r). Taken together, the above results confirmed that NF-κB signaling, cytokine expression, Wnt ligand expression,

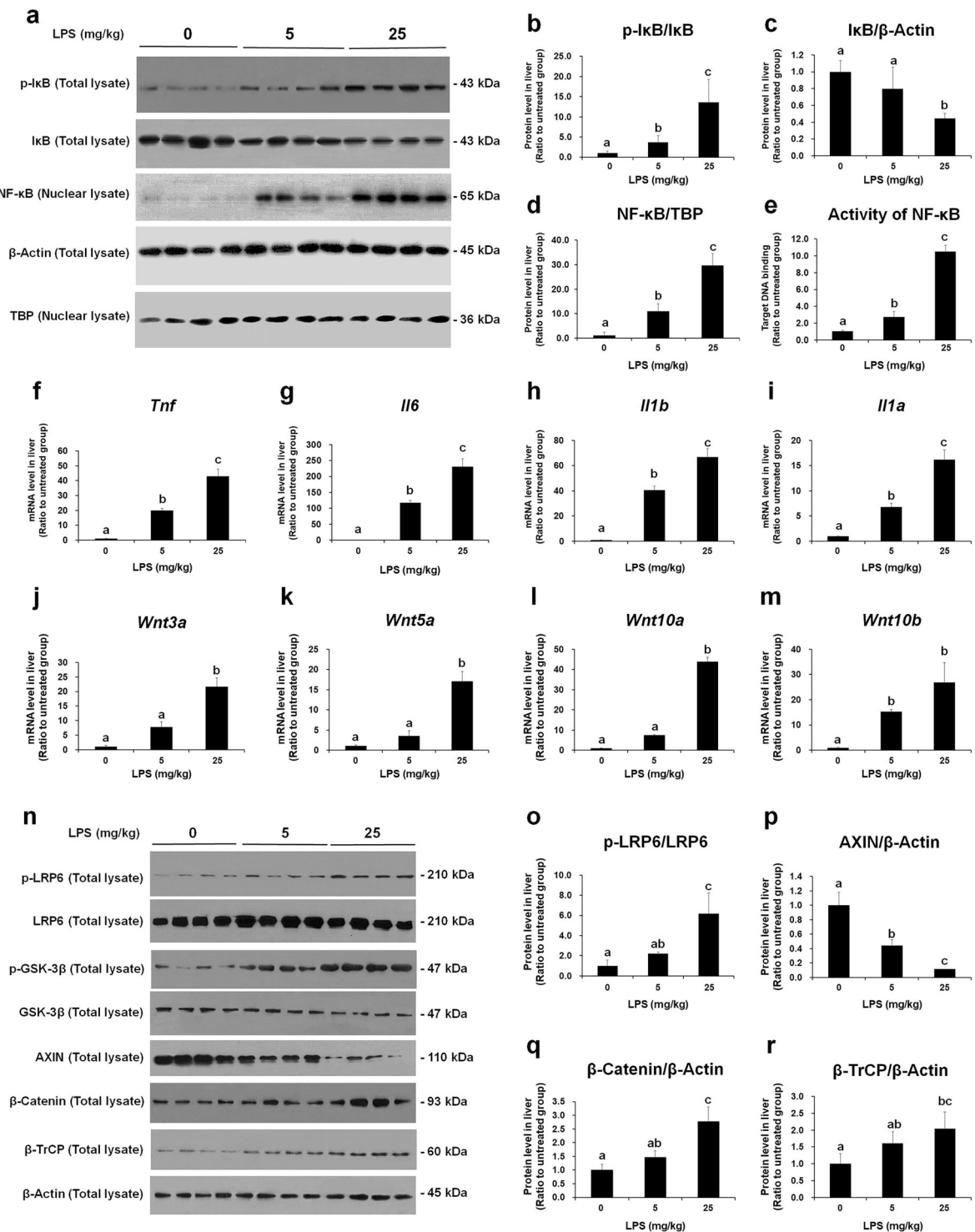


Fig. 4 The NF-κB pathway and Wnt signaling are upregulated in the livers of mice with LPS-induced endotoxemia. Protein and RNA were extracted from the liver tissues of mice injected with 0, 5, or 25 mg/kg LPS. **a** Western blotting was performed to measure the levels of phospho-IkB and IkB in total tissue lysates and the NF-κB protein in nuclear lysates. β-Actin and TATA box-binding protein (TBP) was used as loading controls for total tissue lysates and nuclear lysates, respectively. Western blot raw image data are provided in Supplementary Data 5. **b–d** Band intensities were measured using ImageJ. **e** The binding activity of NF-κB to its target DNA sequence was measured using ELISA. **f–i** Messenger RNA levels of major proinflammatory cytokines was measured by RT-qPCR. **j–m** Messenger RNA levels of Wnt ligands were quantified by RT-qPCR. **n** Levels of the Wnt pathway components were measured by western blotting. β-Actin was used as the loading control. Western blot raw image data are provided in Supplementary Data 5. **o–r** Band intensities were quantified using ImageJ. The data are presented as the mean ± standard deviation values of quadruplicate experiments. Differences among experimental groups were analyzed using one-way ANOVA with Duncan’s multiple range test. The different letters indicate significant differences ($P < 0.05$).

and the Wnt/ β -catenin pathway were upregulated in the livers of mice with LPS-induced endotoxemia. It has been reported that transcripts of some Wnt ligands, including *WNT5A* and *WNT10B*, were induced by NF- κ B^{38–40}, and the promoters of *WNT5A* and *WNT10B* were found to contain NF- κ B-binding sites^{41,42}. We suggest that the LPS-induced Wnt ligand expression and Wnt pathway activation during LPS-induced endotoxemia (Fig. 4j–r) may be attributed to increased NF- κ B signaling and its target DNA binding activity (Fig. 4a–e).

LGK974 suppresses Wnt/ β -catenin signaling, NF- κ B signaling, and cytokine expression in the livers of mice with LPS-induced endotoxemia

We evaluated whether the Wnt signaling inhibitor LGK974 can modulate Wnt/ β -catenin signaling, NF- κ B signaling, and cytokine expression in the livers of endotoxemic mice. Mice were injected *i.p.* with 0 or 60 mg/kg LGK974 and 0 or 25 mg/kg LPS. Protein and RNA were then extracted from the livers of the mice, and the expression of components of the Wnt/ β -catenin pathway was analyzed by western blotting and RT-qPCR. The results confirmed the GSEA data (Fig. 3f), showing that upregulated Wnt signaling in the livers of endotoxemic mice was inhibited by LGK974. The levels of phospho-LRP6 and phospho-GSK-3 β , which were increased by LPS, were significantly reduced after LGK974 treatment (Fig. 5a, b). The total tissue and nuclear levels of β -catenin, the executor protein of the Wnt signaling pathway, were reduced by LGK974 (Fig. 5a, c, d). In addition, the level of β -TrCP, a target gene of β -catenin³⁷, was reduced by LGK974 (Fig. 5a, e). The mRNA levels of *Wnt3a*, *Wnt5a*, *Wnt10a*, and *Wnt10b* in the livers of endotoxemic mice were reduced by LGK974 treatment (Fig. 5f–i). LGK974 alone had no effect on Wnt signaling. The dose-dependent effects of LGK974 on Wnt signaling in the livers of endotoxemic mice are shown in Supplementary Data 6.

Next, using the same liver protein and RNA samples, we analyzed the expression of NF- κ B pathway components and proinflammatory cytokines. The phospho-I κ B level was decreased by LGK974 (Fig. 6a, b). The level of cytoplasmic NF- κ B was increased but that of nuclear NF- κ B was decreased by LGK974 (Fig. 6a, c, d). The binding affinity of NF- κ B for its target DNA was significantly decreased by LGK974 (Fig. 6e), as were the transcript levels of genes encoding proinflammatory cytokines, such as *Tnf*, *Il6*, *Ilb*, and *Il1a* (Fig. 6f–i). When mice were treated with LGK974 alone, no significant changes were observed in this group compared with the saline-treated control group. The dose-dependent effects of LGK974 on NF- κ B signaling and proinflammatory cytokine expression are shown in Supplementary Data 7.

LGK974 reduces the interaction between phospho-I κ B and β -TrCP in the livers of mice with LPS-induced endotoxemia

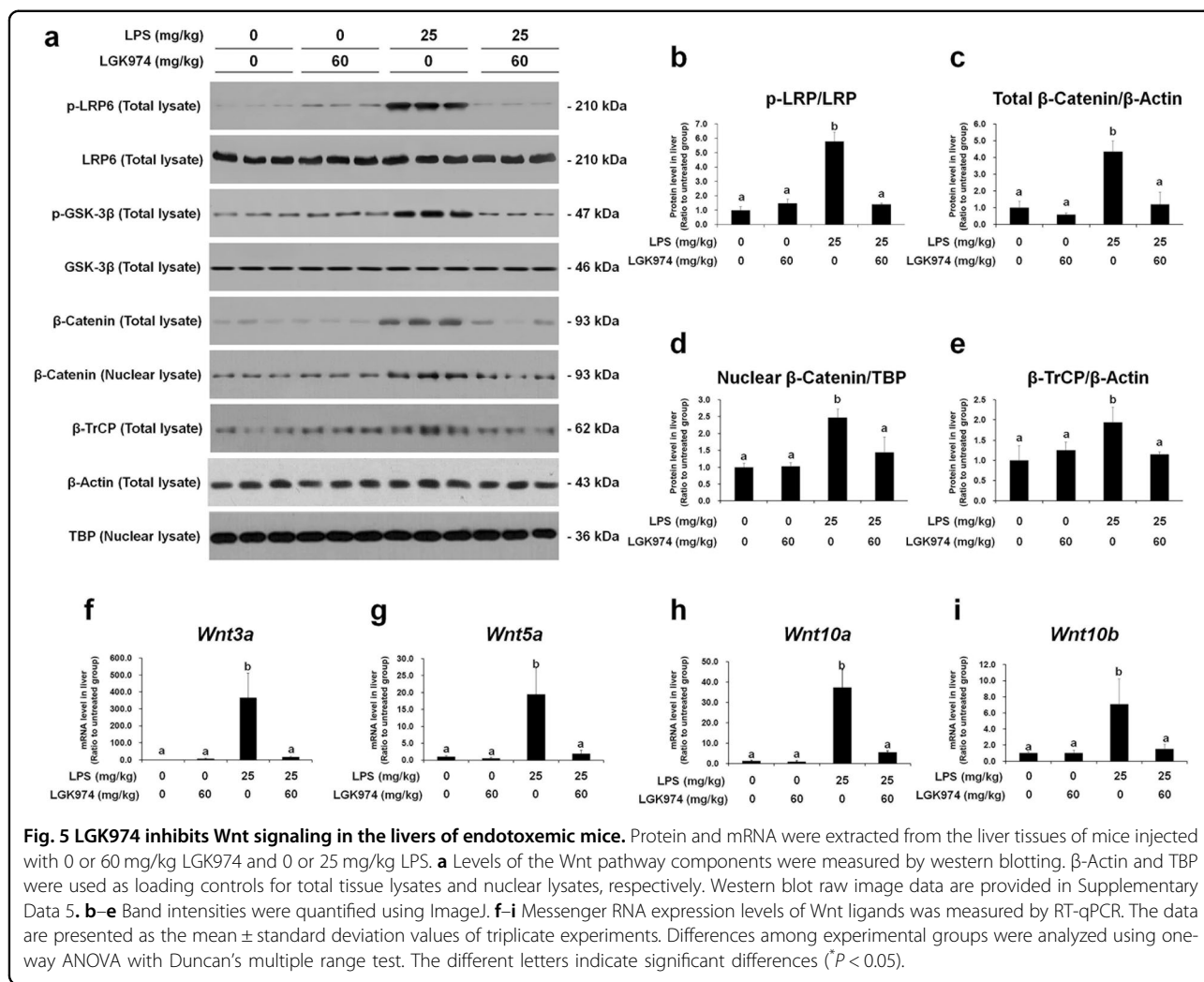
We found that the protein-protein interaction between phospho-I κ B and β -TrCP identified by coimmunoprecipitation was increased in mice with LPS-induced endotoxemia and decreased by LGK974 treatment (Fig. 6j). Western blot analysis of the input samples from the coimmunoprecipitation experiment showed that the protein levels of both β -TrCP and phospho-I κ B were increased by LPS and decreased by LGK974 (Fig. 6k), the same pattern as that shown in Fig. 5e and Fig. 6b. Our data showed that the level of the protein-protein interaction between β -TrCP and phospho-I κ B was proportional to the levels of these proteins in the livers of endotoxemic mice, which were reduced by LGK974.

To date, the interaction between β -TrCP and phospho-I κ B has not been reported in the context of endotoxemia or sepsis. β -TrCP is a component of the I κ B-ubiquitin ligase that induces the ubiquitination of phospho-I κ B^{43–45}; β -TrCP is a rate-limiting mediator that regulates the degradation of phospho-I κ B, with increased binding resulting in increased degradation⁴⁶. We suggest that the increased levels of β -TrCP and phospho-I κ B and the interaction between these two proteins may induce I κ B degradation followed by NF- κ B nuclear translocation and proinflammatory cytokine expression in the livers of endotoxemic mice.

LGK974 reduces the interaction between β -catenin and NF- κ B in the livers of mice with LPS-induced endotoxemia

β -Catenin is the major effector protein of the Wnt/ β -catenin pathway. When this pathway is inactive, β -catenin is phosphorylated by GSK-3 β in a complex containing AXIN and adenomatous polyposis coli (APC) for subsequent proteolysis. Alternatively, when this pathway is active, phosphorylated LRP5/6 recruits AXIN and disrupts the GSK-3 β -AXIN-APC complex, subsequently dephosphorylating and stabilizing β -catenin⁴⁷. Because the levels of the Wnt/ β -catenin and NF- κ B signaling components were modulated by LPS and LGK974, the interaction between β -catenin and NF- κ B was analyzed using coimmunoprecipitation and colocalization experiments. Coimmunoprecipitation of β -catenin and NF- κ B was elevated by LPS; however, it was significantly reduced by LGK974 treatment (Fig. 7a). Data for input samples used in the coimmunoprecipitation assays are shown in Fig. 7b. We also assessed the colocalization of β -catenin and NF- κ B by confocal fluorescence microscopy of liver tissues (Fig. 7c). In saline-treated control mice, β -catenin and NF- κ B did not colocalize ($R = -0.15$); however, in endotoxemic mice, they did ($R = 0.69$), and this colocalization was suppressed by LGK974 treatment ($R = 0.07$).

The interaction between β -catenin and NF- κ B during endotoxemia or sepsis has not been defined to date, even



though recent studies have reported the existence of this interaction in other conditions. It has been reported that overexpression of β -catenin induces nuclear localization of NF- κ B in cardiomyocytes during acute myocardial infarction⁴⁸. In contrast, depletion of β -catenin by siRNA reduces LPS-induced NF- κ B activation in human bronchial epithelial cells⁴⁹. However, it should be noted that the interaction between β -catenin and NF- κ B is complex; β -catenin exerts not only a proinflammatory function by enhancing NF- κ B activity but also an anti-inflammatory function by repressing it. It has been reported that β -catenin reduces NF- κ B activity in human articular chondrocytes⁵⁰. The effect is often cell- and tissue-dependent or stimulus-specific and needs to be investigated in a context-dependent manner⁵¹.

LGK974 reduces liver damage in mice with LPS-induced endotoxemia

We also found that the plasma levels of alanine aminotransferase (ALT) and aspartate aminotransferase

(AST), well-known markers of liver damage, were elevated by LPS and significantly reduced by LGK974 (Fig. 8a, b). In addition, LPS-induced pathological changes in liver tissue, such as necrosis and vacuolation of hepatocytes as well as infiltration of inflammatory cells, were suppressed by LGK974 treatment (Fig. 8c–f).

Recent studies have suggested the involvement of Wnt signaling in sepsis¹⁵. It was reported that the levels of multiple WNT ligands were increased in the peripheral blood of patients with septic shock as well as in splenic tissue of endotoxemic mice¹⁸. WNT5A levels were significantly increased in the sera of patients with sepsis¹⁷ and in lung biopsies from patients with septic acute respiratory distress syndrome⁵². iCRT3, a Wnt signaling inhibitor, reportedly decreased the plasma levels of proinflammatory cytokines and ameliorated lung injury in a mouse model of sepsis induced by cecal ligation and puncture¹⁶. However, the crosstalk between the Wnt/ β -catenin and NF- κ B pathways has not been elucidated in sepsis.

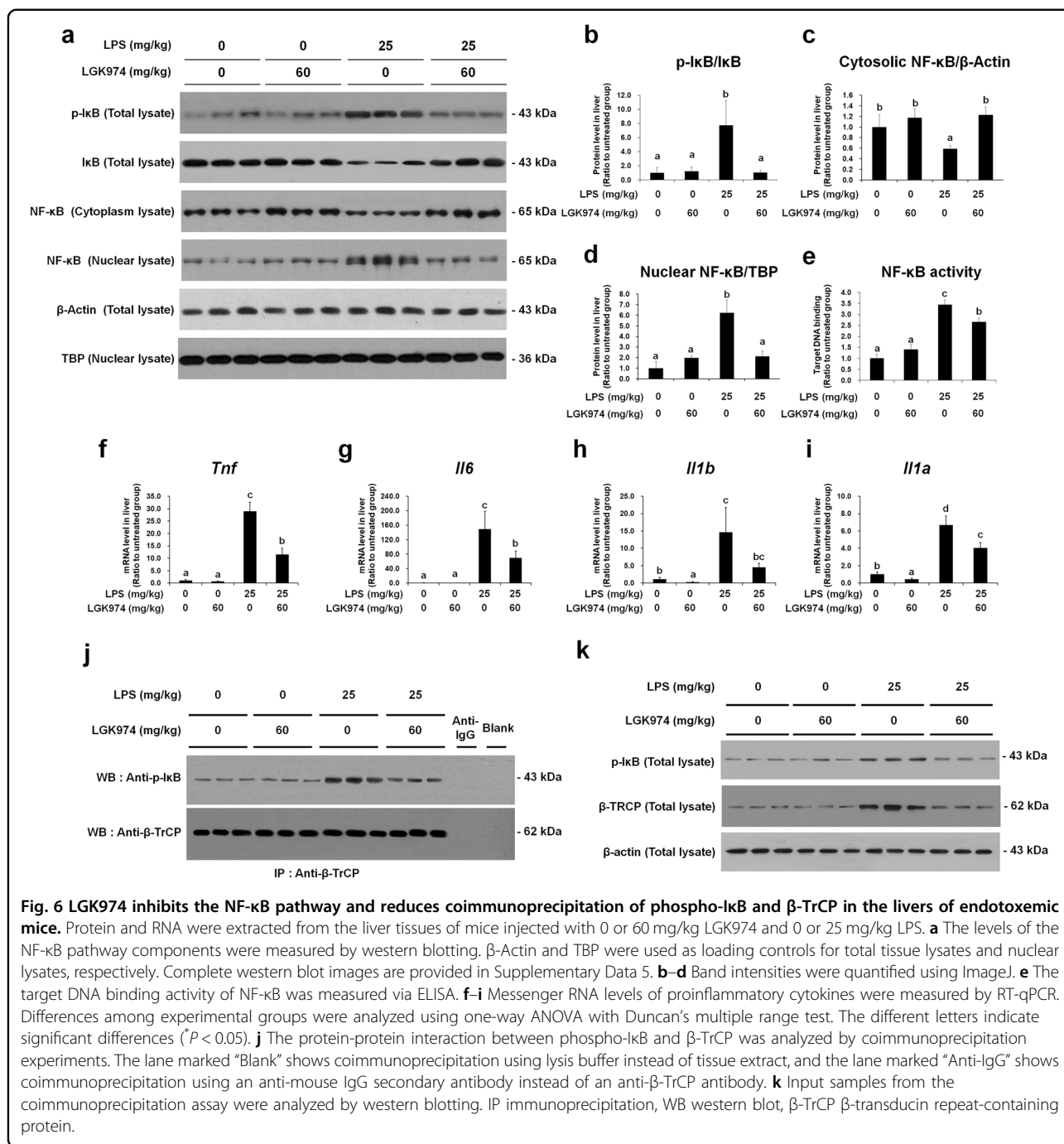


Fig. 6 LGK974 inhibits the NF-κB pathway and reduces coimmunoprecipitation of phospho-IκB and β-TrCP in the livers of endotoxemic mice. Protein and RNA were extracted from the liver tissues of mice injected with 0 or 60 mg/kg LGK974 and 0 or 25 mg/kg LPS. **a** The levels of the NF-κB pathway components were measured by western blotting. β-Actin and TBP were used as loading controls for total tissue lysates and nuclear lysates, respectively. Complete western blot images are provided in Supplementary Data 5. **b–d** Band intensities were quantified using ImageJ. **e** The target DNA binding activity of NF-κB was measured via ELISA. **f–i** Messenger RNA levels of proinflammatory cytokines were measured by RT-qPCR. Differences among experimental groups were analyzed using one-way ANOVA with Duncan's multiple range test. The different letters indicate significant differences ($P < 0.05$). **j** The protein-protein interaction between phospho-IκB and β-TrCP was analyzed by coimmunoprecipitation experiments. The lane marked "Blank" shows coimmunoprecipitation using lysis buffer instead of tissue extract, and the lane marked "Anti-IgG" shows coimmunoprecipitation using an anti-mouse IgG secondary antibody instead of an anti-β-TrCP antibody. **k** Input samples from the coimmunoprecipitation assay were analyzed by western blotting. IP immunoprecipitation, WB western blot, β-TrCP β-transducin repeat-containing protein.

In this study, we identified crosstalk between two pathways in an animal model of sepsis. Our results strongly suggest that the crosstalk between the Wnt/β-catenin and NF-κB pathways contributes to the mutual activation of these two pathways, which results in amplified proinflammatory cytokine production; damage to organs, including the liver; and death. LPS-induced NF-κB signaling may activate the Wnt pathway. Our results showed that the mRNA levels of Wnt ligands,

including *Wnt3a*, *Wnt5a*, *Wnt10a*, and *Wnt10b*, correlated with the target DNA binding activity of NF-κB (Fig. 4e, j–m), as the promoters of some Wnt ligands have binding sites for NF-κB^{38–42}. Wnt ligands, expressed by NF-κB, activated Wnt signaling and increased the levels of both β-catenin and β-TrCP (Fig. 4q, r), subsequently enhancing their protein-protein interactions with NF-κB (Fig. 7a, c) and phospho-IκB (Fig. 6j), which in turn activated NF-κB signaling.

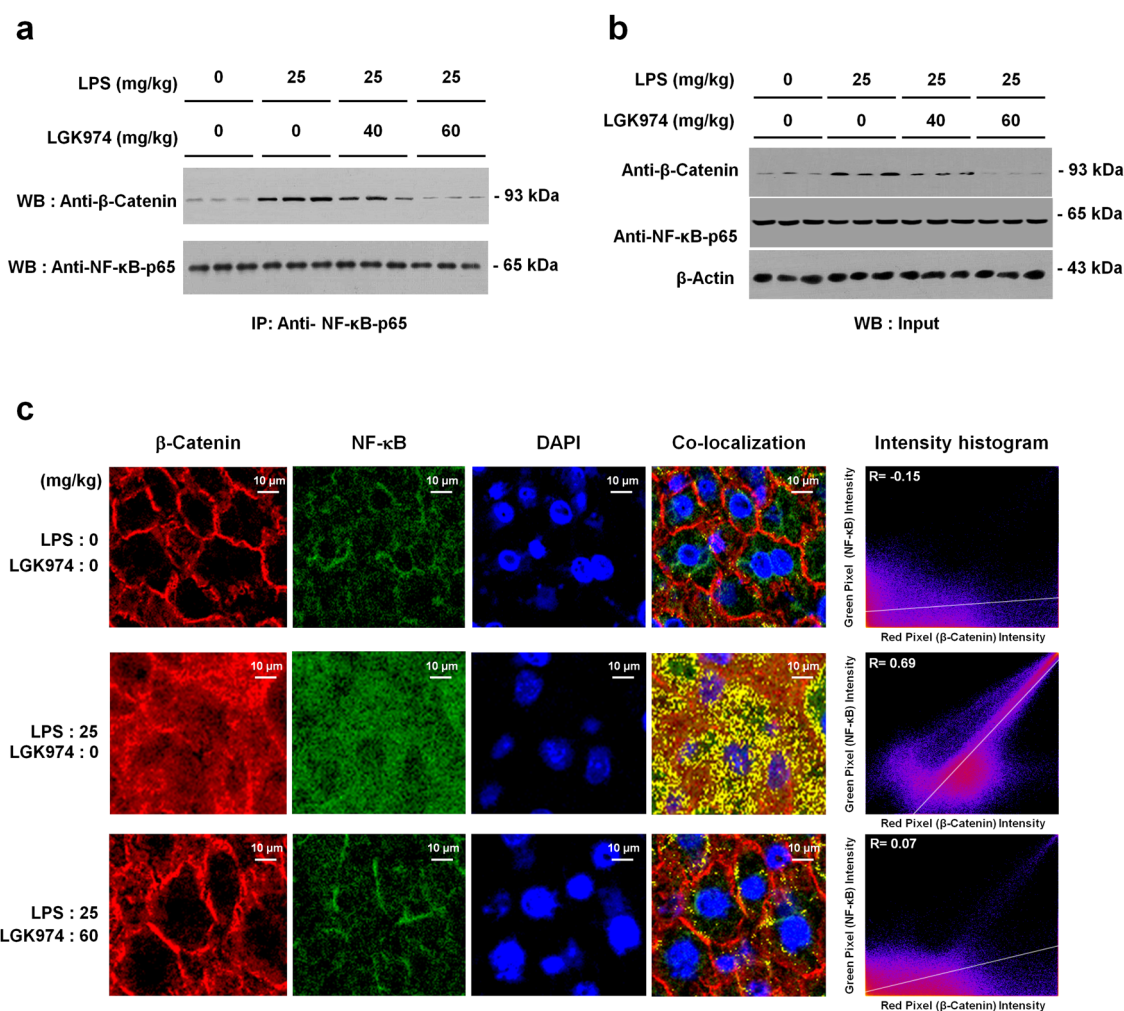


Fig. 7 LGK974 reduces the coimmunoprecipitation and colocalization of β -catenin and NF- κ B in the liver tissues of endotoxemic mice. **a, b** Protein was extracted from the liver tissues of mice injected with 0, 40, or 60 mg/kg LGK974 and 0 or 25 mg/kg LPS. The protein–protein interaction between β -catenin and NF- κ B p65 was analyzed by coimmunoprecipitation (**a**). Input samples from the coimmunoprecipitation assay were analyzed by western blotting (**b**). IP immunoprecipitation, WB western blot. **c** Images showing immunofluorescence staining for β -catenin and NF- κ B and DAPI staining for nuclei. All images were acquired at a magnification of 600 \times using a Nikon Asia confocal system (Nikon, Tokyo, Japan). Images are representative of three experiments. Colocalization was quantified using ImageJ to calculate Pearson correlation coefficient (R) values.

The findings of this study are summarized in Fig. 9. Our experimental data showed LPS-induced NF- κ B signaling and Wnt ligand expression (red lines) as well as increased Wnt/ β -catenin signaling and interactions between β -catenin and NF- κ B and between β -TrCP and I κ B (blue lines). LGK974 exerts a suppressive effect on cytokine production by suppressing the upregulation of β -catenin and β -TrCP as well as their interactions with NF- κ B and phospho-I κ B, respectively. Cytokine-induced NF- κ B pathway activation during sepsis has been documented in previous studies (violet line)⁵³.

We suggest that these interactions may occur in diverse cell types, including endothelial cells and macrophage-type cells in the liver. The liver is considered the main source of cytokine production during

sepsis; Kupffer cells, which are macrophage-type cells in the liver, as well as natural killer cells, CD8⁺ T cells, endothelial cells, hepatic stellate cells, and hepatocytes, have been reported to participate in the production of proinflammatory cytokines during sepsis¹⁴. In our previous study, we showed that LGK974 suppressed proinflammatory cytokine production via modulation of the Wnt pathway in LPS-stimulated human endothelial cells²⁹. Recently, we found that the protein–protein interaction between β -catenin and NF- κ B was enhanced by LPS and reduced by LGK974 in RAW264.7 murine macrophage cells (unpublished observation). In this study, we did not analyze the types of cells in liver tissue, but various cell types, including endothelial cells and macrophage-type cells, may be

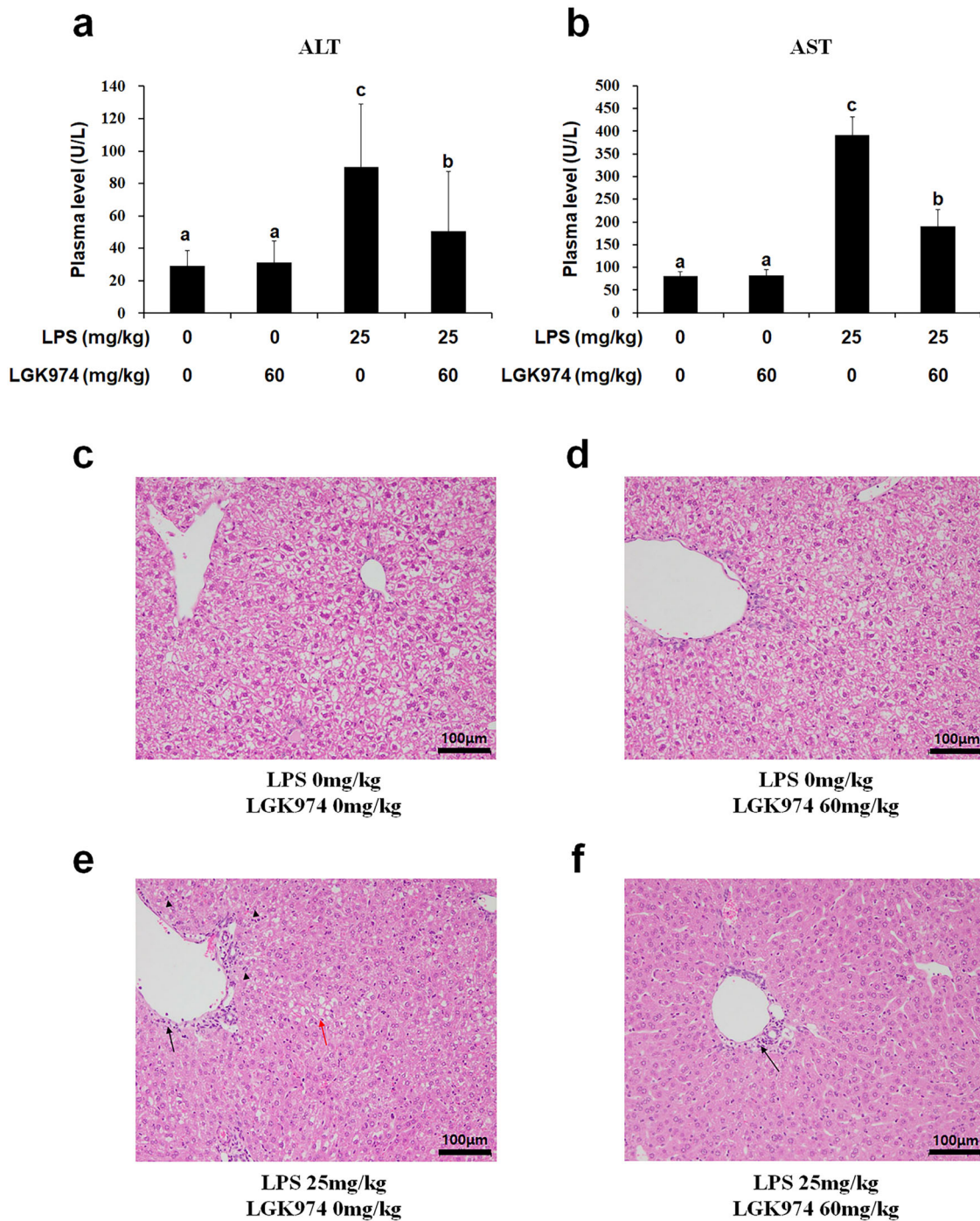
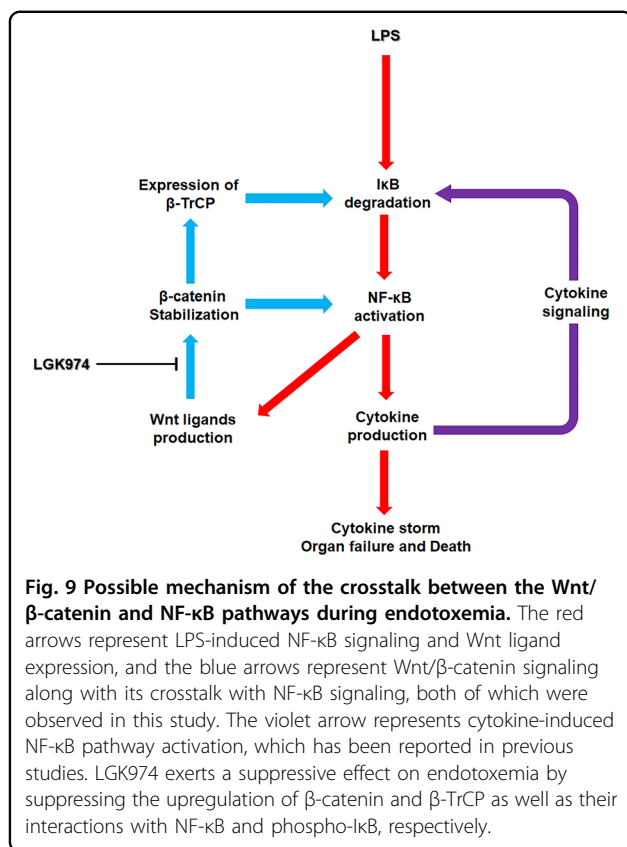


Fig. 8 LGK974 suppressed the increases in ALT and AST levels and the pathological changes in the liver tissue of endotoxemic mice. Plasma and liver tissues were obtained from mice injected with 0 or 60 mg/kg LGK974 and 0 or 25 mg/kg LPS. **a, b** The plasma levels of ALT and AST, well-known markers of liver damage, were measured using a veterinary clinical chemistry analyzer. Differences among experimental groups were analyzed using one-way ANOVA with Duncan’s multiple range test. The different letters indicate statistically significant differences ($P < 0.05$). **c–f** Pathological changes in liver tissues were observed using hematoxylin and eosin staining after formalin fixation. The black arrows indicate inflammatory cell infiltration. The black arrowheads show necrotic cells. The red arrow shows hepatocyte vacuolation. ALT alanine aminotransferase, AST aspartate aminotransferase.



involved in this process. Further study is necessary to confirm the results.

This study has some limitations. We primarily focused on liver dysfunction; thus, further studies are needed to analyze the effects on other organs, such as the lungs, heart, and kidneys. Furthermore, this study focused on the early phase of endotoxemia; most experiments were conducted using liver tissue and blood samples collected 6 h after LPS injection. Further studies are needed to analyze the time course and late phase of endotoxemia. The endotoxin and *E. coli* injection mouse models used in this study have been widely used for sepsis studies to date. As animal models of sepsis only partially recapitulate human sepsis, further studies employing more diverse animal models, including cecal ligation and puncture models, colon ascendent stent peritonitis models, pneumonia models, and implantation models, are needed¹⁰.

In conclusion, we demonstrated that the Wnt signaling inhibitor LGK974 downregulates proinflammatory cytokine production by modulating the crosstalk between the Wnt/β-catenin and NF-κB pathways, thereby suppressing the induction of cytokine storm, liver damage, and lethality in mice with LPS-induced endotoxemia. Our data suggest that LGK974 may be a therapeutic candidate for endotoxemia and sepsis.

Acknowledgements

This research was supported by the Basic Science Research Program (2017R1D1A1B03029033 and 2020R1F1A1064537) of the National Research Foundation (NRF) of Korea. This work was also supported by the Basic Study and Interdisciplinary R&D Foundation Fund of the University of Seoul (2019) to Eek-Hoon Jho. The authors thank eBiogen for assistance with the RNA-seq experiments.

Author details

¹Department of Microbiology, Chung-Ang University College of Medicine, Seoul 06974, Republic of Korea. ²Department of Biochemistry, University of Washington, Seattle, WA 98195, USA. ³Department of Life Science, University of Seoul, Seoul 02504, Republic of Korea

Conflict of interest

The authors declare no competing interests.

Publisher's note

Springer Nature remains neutral with regard to jurisdictional claims in published maps and institutional affiliations.

Supplementary information The online version contains supplementary material available at <https://doi.org/10.1038/s12276-021-00577-z>.

Received: 5 August 2020 Revised: 13 January 2021 Accepted: 24 January 2021.

Published online: 10 March 2021

References

- Danner, R. L. et al. Endotoxemia in human septic shock. *Chest* **99**, 169–175 (1991).
- Chong, D. L. & Sriskandan, S. Pro-inflammatory mechanisms in sepsis. *Contrib. Microbiol.* **17**, 86–107 (2011).
- Chousterman, B. G., Swirski, F. K. & Weber, G. F. Cytokine storm and sepsis disease pathogenesis. *Semin. Immunopathol.* **39**, 517–528 (2017).
- Singer, M. et al. The Third International Consensus Definitions for Sepsis and Septic Shock (Sepsis-3). *J. Am. Med. Assoc.* **315**, 801–810 (2016).
- Kamisoglu, K. et al. Human metabolic response to systemic inflammation: assessment of the concordance between experimental endotoxemia and clinical cases of sepsis/SIRS. *Crit. Care* **19**, 71 (2015).
- Bottiroli, M. et al. Prevalence and clinical significance of early high endotoxin activity in septic shock: an observational study. *J. Crit. Care* **41**, 124–129 (2017).
- Knotek, M. et al. Endotoxemic renal failure in mice: role of tumor necrosis factor independent of inducible nitric oxide synthase. *Kidney Int.* **59**, 2243–2249 (2001).
- Ahmad, A., Gero, D., Olah, G. & Szabo, C. Effect of endotoxemia in mice genetically deficient in cystathionine-gamma-lyase, cystathionine-beta-synthase or 3-mercaptopyruvate sulfurtransferase. *Int. J. Mol. Med.* **38**, 1683–1692 (2016).
- van der Meer, A. J. et al. Neutrophils mitigate the systemic host response during endotoxemia in mice. *Immunology* **156**, 277–281 (2019).
- Kingsley, S. M. & Bhat, B. V. Differential paradigms in animal models of sepsis. *Curr. Infect. Dis. Rep.* **18**, 26 (2016).
- Wang, D., Yin, Y. & Yao, Y. Advances in sepsis-associated liver dysfunction. *Burns Trauma* **2**, 97–105 (2014).
- Enayati, P., Brennan, M. F. & Fong, Y. Systemic and liver cytokine activation. Implications for liver regeneration and posthepatectomy endotoxemia and sepsis. *Arch. Surg.* **129**, 1159–1164 (1994).
- Nesseler, N. et al. Clinical review: the liver in sepsis. *Crit. Care* **16**, 235 (2012).
- Yan, J., Li, S. & Li, S. The role of the liver in sepsis. *Int. Rev. Immunol.* **33**, 498–510 (2014).
- Houshyar, K. S. et al. Role of Wnt signaling during inflammation and sepsis: a review of the literature. *Int. J. Artif. Organs* **41**, 247–253 (2018).
- Sharma, A., Yang, W. L., Ochani, M. & Wang, P. Mitigation of sepsis-induced inflammatory responses and organ injury through targeting Wnt/beta-catenin signaling. *Sci. Rep.* **7**, 9235 (2017).

17. Schulte, D. M. et al. The wingless-related integration site-5a/secreted frizzled-related protein-5 system is dysregulated in human sepsis. *Clin. Exp. Immunol.* **180**, 90–97 (2015).
18. Gatica-Andrades, M. et al. WNT ligands contribute to the immune response during septic shock and amplify endotoxemia-driven inflammation in mice. *Blood Adv.* **1**, 1274–1286 (2017).
19. Liu, J. et al. Targeting Wnt-driven cancer through the inhibition of Porcupine by LGK974. *Proc. Natl Acad. Sci. USA* **110**, 20224–20229 (2013).
20. Boone, J. D. et al. Targeting the Wnt/beta-catenin pathway in primary ovarian cancer with the porcupine inhibitor WNT974. *Lab. Invest.* **96**, 249–259 (2016).
21. Guimaraes, P. P. G. et al. Potent in vivo lung cancer Wnt signaling inhibition via cyclodextrin-LGK974 inclusion complexes. *J. Control Release* **290**, 75–87 (2018).
22. Zimmerli, D. et al. WNT ligands control initiation and progression of human papillomavirus-driven squamous cell carcinoma. *Oncogene* **37**, 3753–3762 (2018).
23. Li, H. et al. Therapeutic effects of antibiotic drug tigecycline against cervical squamous cell carcinoma by inhibiting Wnt/beta-catenin signaling. *Biochem. Biophys. Res. Commun.* **467**, 14–20 (2015).
24. Kahlert, U. D. et al. Pharmacologic Wnt inhibition reduces proliferation, survival, and clonogenicity of glioblastoma cells. *J. Neuropathol. Exp. Neurol.* **74**, 889–900 (2015).
25. Suwala, A. K. et al. Inhibition of Wnt/beta-catenin signaling downregulates expression of aldehyde dehydrogenase isoform 3A1 (ALDH3A1) to reduce resistance against temozolomide in glioblastoma in vitro. *Oncotarget* **9**, 22703–22716 (2018).
26. Picco, G. et al. Loss of AXIN1 drives acquired resistance to WNT pathway blockade in colorectal cancer cells carrying RSP03 fusions. *EMBO Mol. Med.* **9**, 293–303 (2017).
27. Pai, S. G. et al. Wnt/beta-catenin pathway: modulating anticancer immune response. *J. Hematol. Oncol.* **10**, 101 (2017).
28. Li, A. et al. Canonical Wnt inhibitors ameliorate cystogenesis in a mouse ortholog of human ADPKD. *JCI Insight* **3**, e95874 (2018).
29. Jang, J., Jung, Y., Kim, Y., Jho, E. H. & Yoon, Y. LPS-induced inflammatory response is suppressed by Wnt inhibitors, Dickkopf-1 and LGK974. *Sci. Rep.* **7**, 41612 (2017).
30. Mayr, F. B., Yende, S. & Angus, D. C. Epidemiology of severe sepsis. *Virulence* **5**, 4–11 (2014).
31. Subramanian, A. et al. Gene set enrichment analysis: a knowledge-based approach for interpreting genome-wide expression profiles. *Proc. Natl Acad. Sci. USA* **102**, 15545–15550 (2005).
32. Livak, K. J. & Schmittgen, T. D. Analysis of relative gene expression data using real-time quantitative PCR and the 2^{-ΔΔC_T} method. *Methods* **25**, 402–408 (2001).
33. Bae, T. et al. Paeonia lactiflora root extract suppresses cancer cachexia by down-regulating muscular NF-kappaB signalling and muscle-specific E3 ubiquitin ligases in cancer-bearing mice. *J. Ethnopharmacol.* **246**, 112222 (2020).
34. Iyer, S. S. & Cheng, G. Role of interleukin 10 transcriptional regulation in inflammation and autoimmune disease. *Crit. Rev. Immunol.* **32**, 23–63 (2012).
35. Carter, A. B., Monick, M. M. & Hunninghake, G. W. Lipopolysaccharide-induced NF-kappaB activation and cytokine release in human alveolar macrophages is PKC-independent and TK- and PC-PLC-dependent. *Am. J. Respir. Cell Mol. Biol.* **18**, 384–391 (1998).
36. Trede, N. S., Tsytsykova, A. V., Chatila, T., Goldfeld, A. E. & Geha, R. S. Transcriptional activation of the human TNF-alpha promoter by superantigen in human monocytic cells: role of NF-kappa B. *J. Immunol.* **155**, 902–908 (1995).
37. Spiegelman, V. S. et al. Wnt/beta-catenin signaling induces the expression and activity of betaTrCP ubiquitin ligase receptor. *Mol. Cell* **5**, 877–882 (2000).
38. Ge, X. P. et al. Requirement of the NF-kappaB pathway for induction of Wnt-5A by interleukin-1beta in condylar chondrocytes of the temporomandibular joint: functional crosstalk between the Wnt-5A and NF-kappaB signaling pathways. *Osteoarthr. Cartil.* **19**, 111–117 (2011).
39. Blumenthal, A. et al. The Wingless homolog WNT5A and its receptor Frizzled-5 regulate inflammatory responses of human mononuclear cells induced by microbial stimulation. *Blood* **108**, 965–973 (2006).
40. Zhang, Y. et al. Reciprocal requirements for EDA/EDAR/NF-kappaB and Wnt/beta-catenin signaling pathways in hair follicle induction. *Dev. Cell* **17**, 49–61 (2009).
41. Katula, K. S., Joyner-Powell, N. B., Hsu, C. C. & Kuk, A. Differential regulation of the mouse and human Wnt5a alternative promoters A and B. *DNA Cell Biol.* **31**, 1585–1597 (2012).
42. Katoh, M. & Katoh, M. AP1- and NF-kappaB-binding sites conserved among mammalian WNT10B orthologs elucidate the TNFalpha-WNT10B signaling loop implicated in carcinogenesis and adipogenesis. *Int. J. Mol. Med.* **19**, 699–703 (2007).
43. Spencer, E., Jiang, J. & Chen, Z. J. Signal-induced ubiquitination of IkkappaBalpha by the F-box protein Slimb/beta-TrCP. *Genes Dev.* **13**, 284–294 (1999).
44. Winston, J. T. et al. The SCFbeta-TRCP-ubiquitin ligase complex associates specifically with phosphorylated destruction motifs in IkkappaBalpha and beta-catenin and stimulates IkkappaBalpha ubiquitination in vitro. *Genes Dev.* **13**, 270–283 (1999).
45. Shirane, M., Hatakeyama, S., Hattori, K., Nakayama, K. & Nakayama, K. Common pathway for the ubiquitination of IkkappaBalpha, IkkappaBbeta, and IkkappaBepsilon mediated by the F-box protein FWD1. *J. Biol. Chem.* **274**, 28169–28174 (1999).
46. Wang, X., Adhikari, N., Li, Q., Guan, Z. & Hall, J. L. The role of [beta]-transducin repeat-containing protein ([beta]-TrCP) in the regulation of NF-[kappa]B in vascular smooth muscle cells. *Arterioscler. Thromb. Vasc. Biol.* **24**, 85–90 (2004).
47. Cadigan, K. M. & Liu, Y. I. Wnt signaling: complexity at the surface. *J. Cell Sci.* **119**, 395–402 (2006).
48. Lin, J. C. et al. beta-Catenin overexpression causes an increase in inflammatory cytokines and NF-kappaB activation in cardiomyocytes. *Cell Mol. Biol.* **63**, 17–22 (2016).
49. Jang, J., Ha, J. H., Chung, S. I. & Yoon, Y. Beta-catenin regulates NF-kappaB activity and inflammatory cytokine expression in bronchial epithelial cells treated with lipopolysaccharide. *Int. J. Mol. Med.* **34**, 632–638 (2014).
50. Ma, B., van Blitterswijk, C. A. & Karperien, M. A Wnt/beta-catenin negative feedback loop inhibits interleukin-1-induced matrix metalloproteinase expression in human articular chondrocytes. *Arthritis Rheum.* **64**, 2589–2600 (2012).
51. Ma, B. & Hottiger, M. O. Crosstalk between Wnt/beta-Catenin and NF-kappaB signaling pathway during inflammation. *Front. Immunol.* **7**, 378 (2016).
52. Villar, J. et al. Early activation of pro-fibrotic WNT5A in sepsis-induced acute lung injury. *Crit. Care* **18**, 568 (2014).
53. Liu, S. F. & Malik, A. B. NF-kappa B activation as a pathological mechanism of septic shock and inflammation. *Am. J. Physiol. Lung Cell Mol. Physiol.* **290**, L622–L645 (2006).